Seismic slip on the west flank of the Upper Rhine Graben (France-Germany): Evidence from tectonic morphology and cataclastic deformation bands

Zoe K. Shipton[1*], Mustapha Meghraoui[2] and Louise Monro[3]

1. Department of Civil and Environmental Engineering, University of Strathclyde, Glasgow, G11XJ UK. Zoe Shipton <zoe.shipton@strath.ac.uk>
* Corresponding author

2. Ecole et Observatoire des Sciences de la Terre, Institut de Physique de Globe (UMR 7516), 5 rue René Descartes, 67084 Strasbourg, France.
3. Department of Geographical & Earth Sciences, Gregory Building, University of Glasgow, UK, now at Oil Search Limited, Sydney, Australia

4177 words, 39 references, 9 figures.
Running header: Faulting and cataclastic deformation in the Upper Rhine Graben

Abstract.

Intraplate large and moderate earthquakes have occurred along the Upper Rhine Graben (URG) in the past but no coseismic surface faulting has been reported so far. We investigate the 25-km-long linear Riedseltz-Landau normal fault scarp affecting late Pleistocene and Holocene deposits of the western edge of the northern URG. The fault zone with cataclastic deformation textures is exposed in the Riedseltz quarry where it affects Pliocene and late Pleistocene (Wurm) units. Cataclasis is demonstrated by spalling and transgranular fractures in quartz grains concentrated in deformation bands with reduced grain size. The observed microstructures suggest multiple phases of deformation with cataclasis followed by emplacement of Fe-oxide matrix into deformation bands, and later emplacement of a clay-rick matrix into fractures. Previous studies along the fault show late Pleistocene (Wurm) loess deposits and early Holocene sand-silty deposits with 1.5 m and 0.7 m surface slip, respectively. New and previous results provide a minimum 0.15 mm/yr slip rate. A dislocation model suggests a minimum Mw 6.6 earthquake as a plausible scenario in the western edge of northern URG. Surface faulting in young sediments associated with cataclasis provides new evidence for assessing the occurrence of large earthquakes and seismic hazard assessment in the northern URG.

Key words: Upper Rhine Graben, Riedseltz-Landau normal fault, cataclasite, fractured grains.

The Upper Rhine Graben (URG) and Lower Rhine Embayment (LRE) are major intraplate seismically active tectonic zones in the European plate interior with low deformation rates ≤1 mm/yr (Stein et al., 2015). Late Pleistocene and Holocene normal faulting correlated with past earthquake activity and surface ruptures have revealed the potential for Mw ≥ 6.5 earthquakes (Camelbeeck and Meghraoui, 1998; Meghraoui et al., 2001; Vanneste et al.,2001; Ferry et al., 2005; Grützner et al., 2016). Identified fault scarps with cumulative surface slip in the URG and LRE correspond to crustal-scale normal fault structures visible by means of recent seismicity distribution (Bonjer et al., 1984; Camelbeeck and Van Eck, 1994) and seismic reflection data (Brun et al., 1992). In the URG, the active deformation with strain distribution ≤ 10^{-10} and fault slip rate ≤ 0.5 mm/yr can be correlated with a low-level of seismicity (Fig. 1; Ferry et al., 2005; Masson et al., 2010; Fuhrmann et al., 2013). However, major fault segments delineating the graben edges that may generate large intraplate earthquakes are poorly known.

Cataclasis is commonly believed to take place only along faults below depths of 500-1000m (Fulljames et al., 1997; Bense et al., 2003, Petrik et al., 2014). However, recent studies have shown that it is possible to develop cataclasis along faults in shallowly buried unconsolidated sands (Heynekamp et al., 1999; Sigda et al., 1999; Cashman and Cashman 2000; Rawling et al., 2001; Rawling and Goodwin, 2003; 2006; Bense et al., 2003; Cashman et al. 2007; Evans and Bradbury 2007; Saillet and Wibberley 2010) and tuffs (Wilson et al., 2003; 2006). Cashman and Cashman (2000) and Cashman et al. (2007) have suggested that the presence of cataclasis in unconsolidated sand can be used as an indicator of seismic slip. Cashman et al. (2007) showed that at a location where the San Andreas fault is creeping, fault zones cutting unconsolidated sand deform by grain rolling, whereas cataclastic deformation bands are found along segments of the San Andreas fault that have deformed by stick slip in large earthquakes. While deformation bands are not exclusively related to coseismic slip (Balsamo and Storti 2011) the presence of cataclasis in very shallowly buried sediments that have never experienced high confining stress may be an indicator of high dynamic stresses during coseismic slip.

In this study we present evidence for young surface offsets and cataclasis within a fault zone affecting unconsolidated late Pleistocene (loess) and Holocene deposits along the western flank of the northern URG. The Riedseltz-Landau fault zone is exposed in an open pit sand quarry situated about 1.5 km northeast of the town of Riedseltz village, and mapped

using fault scarp morphology crossing late Quaternary alluvial fans. Samples collected from the fault zone in the quarry are analysed for microstructures and mineralogy highlighting the evolution of the cataclastic deformation bands, slip surfaces and fractures. The potential link between coseismic deformation and cataclasis in very shallowly buried unconsolidated sand provides further evidence that this fault has hosted seismic events.

Seismotectonic setting

The NNE-SSW trending Upper Rhine graben (URG) is a section of the European Cenozoic rift system developed in the foreland of the Alps (Fig. 1) and is approximately 300-km long and up to 40 km wide (Illies, 1981). Subsidence and synrift sedimentation initiated in the Eocene due to extension followed by sinistral transtension. Rifting is asymmetric with larger fault displacements, and therefore deeper graben fill, on the eastern side of the northern URG. The thickness of the Quaternary terrestrial clastic sediment sequences is variable with a maximum (200 m) to the Northeast of our study area (Doebel, 1970). The northern URG shows faults with clear geomorphological expression, bounding the footwall blocks of the Black Forest to the east and the Vosges Mountains and Pfalzer Wald to the west (Illies, 1981).

The seismicity of the northern URG region is characterized by low to moderate intraplate seismicity, although damaging earthquakes have occurred in the past (Fig. 1, Bonjer, 1984; Leydecker, 2009; http://www.sisfrance.net). Instrumental and historical earthquakes in the northern URG have apparently not been large enough to cause surface rupture. However the seismogenic layer reaches 20-km-depth and observed fault segment lengths sometimes exceed 20 km (Kervyn et al., 2002), implying a maximum moment magnitude Mw > 6.5 (Leonard, 2010). With regards to the southern URG where the 1356 Basel earthquake (Mw 6.5) can be correlated to a paleoseismic rupture (Meghraoui et al., 2001), the identification of active and seismogenic faults in the northern URG is problematic due to the absence of known large historical earthquakes with surface ruptures. The identification of fault scarps in the area is an issue due to the low slip rates (< 0.5 mm/yr.), dense vegetation cover on mountains and hills, and the high impact of human activity (urban areas and agricultural ploughing) on the geomorphology in valleys. Mapping of faults in the basin has largely been due to seismic reflection and hydrocarbon exploration profiles (e.g., Illies, 1981; Brun et al., 1992; Behrmann et al., 2003). Some studies have focused explicitly on Neogene and Quaternary fault movement with thinning of Quaternary units on the west URG (Haimberger et al., 2005; Peters et al., 2005), though the likelihood of late Pleistocene

and Holocene earthquake activity in the region has increasingly being investigated (Lemeille et al., 1999; Kervyn et al., 2002; Ferry et al., 2005; Nivière et al., 2008; Baize et al., 2013).

The Riedseltz-Landau fault zone

The Riedseltz-Landau fault zone is a north-south trending steep and composite scarp bounding the western flank of the northern URG (Fig. 2a). The fault was not previously identified as an active and seismogenic structure. Seismic profiles (Fig. 2b and c) display normal fault geometry that offset (> 500 m) Oligocene-Miocene units at ~1.5 – 2.0-km-depth. However at the surface the fault appears as a subtle geomorphic lineament structure that separates a higher plateau of basement Hercynian rocks (Vosges Mountains) on the west from lower levels of alluvial fans and fluvial Rhine units to the east. Triangular facets bounding the Vosges Mountain front and cumulative scarps affecting late Quaternary alluvial fans can be traced into the basin along fault scarps. In his neotectonic analysis conducted along the west URG mountain front, Monninger (1985) describes faults in three quarries at Klingenmünster, Barbelroth and Riedseltz affecting upper Pleistocene units with 1.5 to 3.25 m vertical offset. South of Wissembourg, the fault is exposed in the Riedseltz quarry (Lat. 49.00, Long. 7.96), and can be traced for 12-15 km to the south (Fig. 2a and 2c). North of Wissembourg, the fault has two branches with 1) a main strand following the mountain front and extending northward within the basement rocks of the Vosges Mountains until the Leistadt region where it joins the Worms fault scarps (Fig. 2a), and 2) a subtle cumulative scarp located about 3 to 5 km east of the previous fault trace reaching ~20-m-high and affecting late Quaternary alluvial fans immediately west of Landau. North of Landau city and along the mountain front at Forst, Weidenfeller and Zöller (1995) show faulted alluvial deposits and paleosol units with Thermo-luminescence dating spanning from 88 ka to 284 ka. Further north along the west URG border, the fault zone extends for ~70 km and displays two distinct topographic scarps across Wachenheim and Worms regions. Field investigations on the west URG escarpment with tectonic geomorphology (Kervyn et al., 2002) and trenching with radiocarbon dating (Peters, 2007) provide evidence of fault activity between 8 ka and 14 ka. The late Pleistocene and Holocene fault activity is also attested by subsidence observed by Illies and Greiner (1979) and Monninger (1985) who suggest a possible correlation with the 8 October 1952 earthquake (Io VIII MKS; estimated Mw < 5.5; see Fig. 1).

The Riedseltz fault zone exposure

The fault escarpment that cuts late Pleistocene and Holocene units at the surface is exposed at the Riedseltz quarry. Pliocene sandy gravel, is overlain by ~20-m-thick loess (sandy) units, which in turn are overlain by ~10-m-thick sandy-clay deposits. According to BRGM (1977), the loess units belong to the middle and late Quaternary (Riss and Würm glacial classification, respectively), and the alluvial and colluvial sandy-clay units are Holocene (Fig. 2d). The fault zone exposed in quarry is also visible in shallow (0 to 5-m-depth) geophysical data (Ground Penetrating Radar, seismic reflection, seismic refraction and electrical resistivity profiles from Bano et al., 2002). Bano et al. (2002) report that the fault cuts the boundary between Pliocene sands and the overlying loess-alluvial units with a total vertical offset of ~1.5 m along a fault oriented 165/60E. The quarried face trends approximately east-west, exposing an east-dipping fault zone in cross section (Fig. 3a). The bedding in the lower sand unit is obviously cut off against the fault and bedding dip steepens into the fault zone. Due to the quarry activity, the footwall of the fault is almost entirely covered with quarrying debris so sedimentary units could not be correlated across the fault. Bano et al. (2002) used the shallow geophysical profiles to trace the fault for 50 m to the north and 750 m to the south of the exposed cross section and showed that in the southern half of the quarry the fault splits into two strands both of which offset the Loess and overlying alluvial stratigraphy.

Consistent with observations of Monninger (1985), the fault is comprised of a central zone of relatively structureless, mottled, mixed sand bounded on either side by localised fine-grained, clay-rich and iron stained slip-surfaces (Fig. 3b). The width of this mixed zone is variable, narrowing from 70 cm at the top of the exposure to 20 cm at the base over a distance of 2 metres. The slip-surfaces are covered in a veneer of clay up to 5 mm thick that is sometimes rather patchy. The main fault zone also contains closely spaced deformation bands (Fig. 4a and b). In the hangingwall, pale deformation bands that offset bedding by up to 1 cm are distributed around the fault core to a distance of 1.10-1.15 m. These deformation bands have rather irregular traces when compared to bands formed in well-cemented sandstones (e.g. Fossen et al. 2007). The sand within the fault zone is variably stained bright yellow, orange and brown. The boundaries between different alteration colours are very sharp where clay-rich slip surfaces occur, but are more diffuse elsewhere. Deformation bands also act as abrupt boundaries for the colour variations in the host sandstone. Dark brown and black Fe-oxide concretions are particularly concentrated along the slip surfaces.

Measurements of excavated slip surfaces show steep dip to the east with a mean of 181/72E (inset, Fig 3) consistent with the geophysical observations of Bano et al. (2002).

When the outcrop is carefully excavated to show a view onto the slip-surface face it can be seen that the oxide mineralisation appears to have been streaked out, which may be a proxy for slickenlines (Fig 4b). Due to the looseness of the deposits it was not possible to take accurate slip vector measurements but the streaks are oriented in the down dip direction, consistent with normal faulting.

Deformation bands and microfractures in the fault zone

Determining if these faults have cataclastic microstructures similar to those that Cashman et al. (2007) link to seismic activity requires a detailed study of the host sediments and the deformed fault rocks. Specimens of the undeformed host sediment (late Pleistocene loess) were sampled using hand-tools to scoop out the almost completely unconsolidated sand. Lumps of the more consolidated, and therefore more easily sampled, fault sand were broken off with hand tools and tightly wrapped in duct tape to preserve the sample integrity for thin sectioning. Samples were impregnated with resin in a vacuum chamber before curing. The morphology of the deformed sand was observed in thin section using an optical microscope and SEM, and by 3D grain analysis on the SEM. Friable samples are dried in the oven at 60°C for 2-3 hours. They are then coated with Buehler EpoHeat epoxy resin and returned to the oven for 2-3 hours for the resin to cure. The sample is sliced to approximately 1cm, and again dried for 1-2 hours before being treated again with resin and set again before preparing the thin section.

The host sediments are fine to medium grained, moderately well sorted and sub-rounded sands. They are cross-bedded with occasional metre thick coarse-grained incised channels. The sand consists of 70% single crystal or polycrystalline quartz grains, with 20% lithic grains and 10% feldspar (from CL analysis). Strained quartz grains are common with undulose extinction and mylonitic fabrics, consistent with a metamorphic source for much of the sediment. The host sand grains range from sub-angular to rounded. Quartz overgrowths are occasionally seen but their irregular distribution and the high clay content of the matrix suggests that these may have been reworked from older, more cemented sand into these sediments. Occasional oxide-cemented lithic grains are also likely to have been reworked. Throughout the quarry the sands have been stained a variety of shades of pale yellow to orange (Fig. 3b). The colour banding can be seen to cross cut the bedding in the host sands (e.g. Fig. 3b – bottom left hand corner) so the staining is therefore post-depositional. From sieving and thin-section analysis the maximum grain size in both the host sand and the

deformed sand is ~ 1 mm. The modal grain size of the host sands determined by sieving range from 0.25mm to 0.125mm.

The deformation bands are localised zones of significant grain size reduction a few mm wide that contain highly angular grains (Fig. 5a, b and c). These zones still contain rounded grains but these are mostly over 0.25mm in diameter and the smaller grains (<0.25mm) show significantly more angularity than in the host rock. The preservation of 'survivor grains' surrounded by more angular fragments is a common feature of cataclastic deformation bands. Many of the quartz grains have fresh conchoidal fractures at the edge of the grain. These appear as elongate flakes of quartz, with some partially attached to the grain (Fig. 6). This is similar to the grain spalling reported by Rawling and Goodwin (2003), which is diagnostic of grain fracturing under low confining pressures. Some transgranular fractures are also preserved. The deformation band zones clearly have reduced porosity with respect to the host rock (Fig. 5c). The striking colouration of the deformation zone observed in Figures 3, 5 and 7 is due to a strongly coloured matrix in the fault zone rocks. Matrix colour ranges from bright orange to black and each matrix type has a consistent proportion of fine grains (<0.05mm). The orange matrix contains streaks of yellow and brown colours in plain polarized light (Fig. 7a), while in cross-polarized light it has medium to high birefringence colours. A major character of the orange matrix is its 'flowing' appearance (Fig. 7b) and it often mixes with a less obvious matrix that mostly consists of fine grains. The black matrix is opaque and contains few to no fine grains. In thin section the black matrix often appears fractured with some of these fractures being filled by the orange matrix (Fig. 7c). Within the black matrix the grains are dominantly sub- angular to angular and are mostly >0.25mm with very little finer grains (<0.05mm) and a notable lack of grain contacts (Fig. 7d). The grains here, regardless of size, appear to be largely sub-angular to angular throughout, with only a few grains appearing to be rounded. In these matrix-supported zones have up to 40% black matrix.

Geochemical element spot analysis on the SEM shows that the orange matrix is dominated by clays while the black matrix is predominantly Fe-rich oxide (Fig 8). XRD analyses of three sets of powdered samples (hangingwall, footwall and fault zone) show that, in agreement with the microstructural observations, quartz dominates the XRD diffraction patterns to the extent that other minerals cannot be identified. Results for the clay size fraction (<2μm) show little variation in clay composition between the samples within the fault and those outside the fault (Fig. 9). The dominant peaks are 12.3 and 24.9 2θ, which indicates kaolinite, although Fe-chlorite cannot be ruled out as these are difficult to distinguish in

mixtures using XRD. These peaks are consistently reduced within the fault zone compared to the host sand. All samples show a 10Å mica (muscovite), though this is less pronounced in samples from the fault zone. Samples 0401, 0402, 0407 and 0409 contain some <2μm quartz (identified from the 20.92 second order peak), but it is likely that all samples contain some amount of <2μm quartz. Minor peaks suggest the presence of halite and hydroxysodalite. No significant peak shifts were seen in glycolated <2μm slides indicating that expandable minerals are absent or insignificant in these samples.

On the seismic character of the Riedseltz-Landau fault: A discussion

The Riedseltz-Landau fault zone appears as a major tectonic structure of the western flank of the northern Upper Rhine Graben. The total fault length from Soultz in France to Worms in Germany reaches ~85 km and it may be subdivided in three segments: 1) the Riedseltz segment from Soultz to Landau (~35 km) and along the Vosges Mountain front with a 25-km-long parallel eastern Landau fault branch to the east, 2) the Lambrecht segment from Landau to Leistadt that stretches for ~34 km through the pre-Permian basement rock, and 3) the Worms segment from Leistadt to Wachenheim extending 16 km across the Quaternary alluvial fan deposits. Although of moderate magnitude (Mw < 5.5), the western edge of the northern URG has been the site of recurrent earthquake activity such as the 1952 earthquake sequence (24/02 Io VI, 29/09 Io VI and 08/10/ Io VII, Fig. 1). In addition to our field observations from the Riedseltz quarry, surface fault slip affecting late Pleistocene and Holocene deposits along the fault zone by Illies and Greiner (1979), Monninger (1985) and Peters (2007) support the seismogenic nature of the Riedseltz-Landau fault zone.

The cataclastic structures in the fault zone suggest more than one episode of deformation, based on cross cutting relationships between fault rocks with different matrix compositions. The earliest event (or events) was an episode of shearing that crushed grains, resulting in an increase in angularity of the grains in the fault zone. Coeval or subsequent dilation permitted the introduction of the prominent Fe-oxide matrix into the deformation bands. A possible explanation for the lack of fine grains and the spacing between the existing grains is that while the matrix was infilling the space created by the dilation, it flushed out the fine grains, leaving behind only the larger grains. A subsequent fracture event produced more fine grains and allowed clay matrix introduction into the deformation bands (Fig. 7 d). In this most recent phase of deformation the fine grains were not flushed out, this may be due to a

lack of dilation or due to different hydrological conditions and the fault acting as a barrier to lateral flow. Faults in unconsolidated sediments in the lower Rhine Embayment have been shown to exhibit similar behaviour (Bense and Van Balen 2004). Bense et al. (2003) suggest that Fe-oxide enrichment in faulted sand can be caused by repeated wetting and drying during fluctuations in water table. They observe that oxides are preferentially precipitated along fine-grained laminae, which will have a higher capacity to retain water by capillary action. Incidentally, Behrmann et al. (2003) suggest that ongoing seismic slip along faults in the Rhine Graben may have reduced the efficacy of oil and gas seals by brecciation and fracturing of previously good fault seals, thereby reducing the overall hydrocarbon potential of the area.

Cashman and Cashman (2000), Cashman et al. (2007) and Balsamo and Storti (2011) have suggested that the presence of cataclasis in shallow, unconsolidated sand, where the overburden pressure should be very low, is an indicator of deformation during seismic slip. The Riedseltz fault has comparable structures to other reports of faulted unconsolidated sediment. A similar central mixed zone surrounded by deformation bands is observed by Haynekamp et al. (1999) and Rawling et al. (2001) in the Rio Grande Rift intraplate region. The fault described by Rawling and Goodwin (2003), which was deformed at burial depths up to 1km, contained a much more intense zone of deformation bands than the Riedseltz fault. Cashman and Cashman (2000) report grain crushing in deformation bands cutting sediments buried as little as 50m (equivalent to 1MPa). Conversely, the fault reported by Balsamo and Storti (2011) cutting did not contain any deformation bands, however it did contain grains deformed by spalling and transgranular fracturing as well as mineralogical changes consistent with heating during coseismic slip (c.f. Balsamo et al. 2014).

In the western edge of the northern URG, the maximum thickness of overburden at the time of faulting is unknown and it is possible that the sand could have been eroded prior to deposition of the loess. The potential maximum thickness of Quaternary sediments (225 m at the depocentre east of Worms) drawn from the isopach map (Haimberger et al., 2005), suggests that the Quaternary sediments thin towards the southwest to less than 20m close to Riedseltz. Therefore the maximum likely overburden for these sands is of the order of a few tens of metres. This is at least as shallow as previously reported cataclastic faults in unconsolidated sands. If the hypothesis of Cashman and Cashman (2007) stands then it is probable that the deformation bands and slickenlines from the exposed fault at the Riedseltz quarry may record one or more seismic slip events.

Critical state soil mechanics can be used to constrain the overburden required for localised failure, cataclasis and porosity reduction (Schultz and Siddharthan, 2005). A failure

envelope defined by the mean grain size and porosity of the host sediments constrains whether dilation or compression is the dominant means of deformation. Critical state soil mechanics combines a failure envelope with a critical state line which makes it possible to constrain whether dilation or compression is the dominant means of deformation. The mean grain size determined by sieving was 0.2 ±0.1 mm and the modal grain size of the host sand is 125-250 μm. As no intact host sediment samples were collected, we base the porosity estimates on that for unconsolidated, poorly sorted sands (25% to 35%). The porosity represented by the Fe-oxide matrix is very high (>40%), whereas the areas that appear crushed have very little obvious porosity (<10%).

Cuss et al. (2003) experimentally determined a yield envelope for Penrith sandstone (grain size 129 ± 30 μm and porosity of 28%) that is appropriate to model the stresses required to produce the observed structures at Riedseltz. Using the Penrith sandstone yield envelope, producing the earlier dilation phase of deformation would require a change in the effective mean stress and the differential stress as a result of either a decrease in pore fluid pressure or an increase in overburden. The conditions to produce the later formed deformation bands would require an effective mean stress of >75 MPa and a differential stress of <80 MPa. However, if the maximum likely overburden at the site is 20m, the maximum confining pressure would only have been 0.4 MPa. An overburden equivalent to 3km is required to produce the 75 MPa effective mean stress to develop the deformation bands present in the Riedseltz samples. As these conditions are highly unlikely, a more plausible means would be to produce the localised zones of cataclasis during seismic movement, i.e. by dynamic stress changes rather than quasi-static loading through burial.

Distinguishing between structures that were produced by seismic slip and/or by aseismic creep has critical implications for the seismic hazard analysis. This is even more difficult when dealing with fault scarps in intraplate tectonic domains with high vegetation cover as in the Rhine graben, and where fault slip rates do not exceed 0.3 mm/yr (Camelbeeck and Meghraoui, 1998; Camelbeeck et al., 2007). The 1952 earthquake sequence of the western flank of the northern URG occurred immediately west of Wissembourg - Worms fault scarp Riedseltz (Fig. 1, Illies, 1981; Helm, 1995; Leydecker, 2009) suggesting that Riedseltz normal fault may be associated with a seismically active fault at depth. Here, we speculate on the likelihood of seismic slip along the Riedseltz fault and the magnitude of any earthquakes that may have happened on it.

The Riedseltz normal fault is oriented NNE and it is under extension according to the NE-SW extensional stress field from focal mechanisms (Plenefisch and Bonjer 1997) and

field observations (Bano et al., 2002; Kervyn et al., 2002). If the total vertical offset of 1.5m was the maximum slip in a single event it would represent an earthquake of magnitude up to Mw 6.8 (see figure 9 in Leonard, 2010). Another scenario is that the 1.5 m fault slip is cumulative and represents more than one earthquake and may even include postseismic movement or creep. Taking into account the observed youngest, normal fault scarp heights (average 0.6 m and about half of the slip observed by Bano et al., 2002 in geophysical profiles) in Riedseltz and along the Landau – Worm fault section, the 70-80 east dipping ~25-km-long fault (red arrows in Fig. 2b, fault dip also visible in seismic profile of Fig. 3c) and 15-km-thick seismogenic layer, a simple dislocation model (Okada, 1985) suggests a minimum seismic moment of 9.2 10^{18} N.m , equivalent to Mw 6.6 (Fig. 8). As observed in the Riedseltz quarry (this study), on geophysical profiles by Bano et al. (2002), in the Klingenmünster and Barbelroth quarries (Monninger, 1985), and inferred from the geological map (Fig. 3d; BRGM, 1977), the fault affects Würm loess overlaid by Holocene alluvial sandy-gravel (younger than *ca* 24 ka before present according to the geological map; BRGM, 1977). The 1.5 m – 3.25 m vertical slip must be younger than 24 ka, giving a minimum time-averaged slip rate of 0.15 – 0.32 mm/yr. These slip rates compare well to those for other faults in the Rhine Graben system (Camelbeeck et al., 2007). Ferry et al., (2005) and Nivière et al. (2008) examined river terraces in the southern URG and concluded that vertical fault slip rates varied from 0.1 to 0.3 mm/yr. Although these slip rates fall within the values for seismically active faults, it is not necessary that this slip occurred all in one event. Although fault structures, deformation bands and scarp morphology all suggest one or more events with coseismic slip with a minimum 5000 years recurrence interval (estimated from 0.6 m average coseismic slip) for earthquakes with Mw ≥ 6.6, aseismic slip with creep movement cannot be ruled out.

Conclusions

The Riedseltz-Landau fault is identified as a major active segment of the western flank of the northern Upper Rhine Graben. The Riedseltz fault segment 25-km-long and appears as a linear strand at the frontal topography of the Vosges Mountains showing prominent triangular facets and affecting late Quaternary alluvial and fluvial deposits. The fault affects late Pleistocene and Holocene alluvial units (Illies and Greiner, 1979; Monninger, 1985; Weidenfeller and Zöller, 1995; Peters, 2007) and shows about 1.5 m slip in shallow geophysical profiles (Bano et al., 2002). Field investigations on fault scarp morphology

combined with the study of the fault exposure in the Riedseltz quarry indicate repeated cataclastic slip and fracturing on a narrow zone of deformation.

Detailed microstructure and mineralogical studies of the fault cataclasite using the analysis of SEM and XRD images indicate deformation bands in mixed zones with low grain size and slip surfaces with grain size reduction and streaked out bands due to oxide concentration. The deformation bands also appear with highly fractured grains showing spalling and transgranular fractures in quartz that illustrate the intense shearing and the possible seismic slip in the fault zone. The fault structures and related cataclasis suggest two phases of deformation with 1) shearing, grain crushing and porosity reduction within deformation bands 2) emplacement of the prominent Fe-oxide matrix into the fault zone, possibly accomplished by flushing out of fine grains, and 3) at least one further fracturing episode producing more fine grains and allowing clay matrix emplacement. The presence of cataclastic deformation bands shows that that localized failure occurred despite the minimal overburden (< 20m). Cataclasis could be a very helpful indicator for seismic slip in shallowly buried sediments but more work is required to further constrain the micromechanics of cataclasis under very low confining stress.

The fault scarp and surface deformation bands may be related to successive seismic slip but we cannot rule out the existence of aseismic slip. Further paleoseismic investigations are required to determine the relative amounts of seismic and aseismic slip along the Riedseltz-Landau fault segment. For the moment, a simple fault model suggests a minimum Mw 6.6 earthquake as a plausible scenario for seismic slip along the western edge of the northern Upper Rhine Graben.

Acknowledgements

We thank Kenny Roberts, Peter Chung John Gilleece and Caroline Smith for their technical expertise; Matthieu Ferry, Tony Nemer, Pierre-Jean Alasset and Justin Erickson for field assistance; Martin Lee and Colin Braithwaite for assistance with sedimentary structures. XRD samples were prepared and run by Robbie Goodhue of Trinity College, Dublin. We thank Kurt Decker and Ramon Arrowsmith for their review of manuscript. Collaboration between ZKS and MM was facilitated by the EOST-IPGS (CNRS-UMR 7516) visitor programme and the Ulysses Ireland-France EGIDE-CAMPUS research visit scheme.

411

412 **References**

413 Baize, S., Cushing, M., Lemeille, F., Jomard, E. 2013. Updated seismotectonic zoning scheme
414 of Metropolitan France, with reference to geologic and seismotectonic data. Bull. Soc.
415 geol. Fr., 184, n°3, 225-259.

416 Balsamo F. and Storti, F. 2011. Size-dependent comminution, tectonic mixing and sealing
417 behaviour of a "structurally oversimplified" fault zone in poorly lithified sands: Evidence
418 for a cosesimic rupture? Geological Socuety of America Bulletin, 123, p. 601-619. doi:
419 10.1130/B30099.1

420 Balsamo, F., Aldega, L., De Paola, N., Faoro, I. & Storti, F. (2014). The signature and
421 mechanics of earthquake ruptures along shallow creeping faults in poorly lithified
422 sediments. Geology 42, 435-438. doi: 10.1130/G35272.1

423 Bano M., Edel J.-B., Herquel G. and EPGS Class 2001-2002. 2002. Geophysical investigation
424 of a recent shallow fault. The Leading Edge, 21, 648-650. doi: 10.1190/1.1497317

425 Behrmann J. H., Hermann O., Horstmann M., Tanner D.C., and Bertrand G. 2003. Anatomy
426 and kinematics of oblique continental rifting revealed: A three-dimensional case study of
427 the southeast Upper Rhine graben (Germany). AAPG Bulletin, 87, 1105–1121.

428 Bense V. F. and Van Balen, R. T. 2004. The effect of fault relay and clay smearing on
429 groundwater flow patterns in the Lower Rhine Embayment. Basin Research, 16, 397–411.

430 Bense, V.F., Van den Berg, E.H., Van Balen, R.T. 2003. Deformation mechanisms and
431 hydraulic properties of fault zones in unconsolidated sediments; the Roer Valley Rift
432 System. The Netherlands Hydrogeology Journal, 11, 319-332.

433 Bonjer, K.-P., Gelbke, C., Gilg, B., Rouland, D., Mayer-Rosa, D., Massinon, B. 1984.
434 Seismicity and dynamics of the Upper Rhine graben. Journal of Geophysics 55, 1–12.

435 BRGM, 1977, Carte Géologique Seltz-Wissembourg (1/50 000), N°199, Bureau de Recherche
436 Géologique et Minière, 75015 Paris, France.

437 Brun, J. P., Gutscher M. A. and DEKORP-ECORS teams. 1992. Deep crustal structure of the
438 Rhine Graben from DEKORP-ECORS seismic reflection data: a summary.
439 Tectonophysics, 208, 139-147.

440 Camelbeeck T, and Van Eck T. 1994. The Roer Valley Graben earthquake of 13 April 1992
441 and its seismotectonic setting, Terra Nova, 6, 291-300.

442 Camelbeeck T, Meghraoui M. 1998. Geological and geophysical evidence for large
443 paleoearthquakes with surface faulting in the Roer Graben (northwest Europe). Geophys.
444 J. Int., 132, 347-362.

445 Camelbeeck, T., Vanneste, K. et al. 2007. Relevance of active faulting and seismicity studies
446 to assess longterm earthquake activity in Northwest Europe. In: Stein, S.&Mazzotti, S.
447 (eds) Continental Intraplate Earthquakes: Science, Hazard, and Policy Issues. Geological
448 Society of America, Special Papers, 425, 193–224.

449 Cara, M., Cansi, Y., Schlupp, A. et al. 2015. SI-Hex: a new catalogue of instrumental
450 seismicity for metropolitan France. Bull. Soc. géol. France, t. 186, no 1, 3-19,
451 doi:10.2113/gssgfbull.186.1.3.

452 Cashman, S., Cashman, K. 2000. Cataclasis and deformation formation in unconsolidated
453 marine terrace sand, Humboldt County, California. Geology, v. 28, no. 2, 111-114.

454 Cashman S.M., Baldwin J. N., Cashman K.V., Swanson K. and Crawford R. 2007.
455 Microstructures developed by coseismic and aseismic faulting in near-surface sediments,
456 San Andreas fault, California. Geology, 35, 611–614; doi: 10.1130/G23545A.1

457 Doebl, F. 1970. Die tertiären und quartären Sedimente des südlichen Rheingrabens. In: Illies,
458 J.H., Mueller, S. (Eds.), Graben Poblems. Proceedings of an International Rift
459 Symposium held in Karlsruhe October, 10–12, 1968. E. Schweizerbart'sche, Stuttgart,
460 56–66.

461 Evans, J. P., & Bradbury, K. K. 2007. Fractured dirt: Deformation textures and processes in
462 sediment and other unconsolidated deposits. *Geology*,*35*(7), 671-672.

463 Farr, T.G., Kobrick, M. 2000. Shuttle Radar Topography Mission produces a wealth of data.
464 Eos. Trans. AGU, 81, 583–585.

465 Ferry M., Meghraoui M., Delouis B. and Giardini D. 2005, Evidence for Holocene
466 Paleoseismicity along the Basel-Reinach Active Normal Fault (Switzerland): A Seismic
467 Source for the 1356 Earthquake in the Upper Rhine Graben. Geophys. J. Int., 158, 1-21.

468 Fossen H., Schultz R. A., Shipton Z. K. and Mair K. 2007. Deformation bands in sandstone –
469 a review. Journal of the Geological Society, 164, 755–769.

470 Fuhrmann, T., Heck, B., Knöpfler, A., Masson, F., Mayer, M., Ulrich, P. Westerhaus, M.,
471 Zippelt, K. 2013. Recent surface displacements in the Upper Rhine Graben - Preliminary
472 results from geodetic networks. Tectonophysics, 602(0), 300–315.

473 Grützner, C., Fischer, P. and Reicherter, K., 2016. Holocene surface ruptures of the Rurrand
474 Fault, Germany—insights from palaeoseismology, remote sensing and shallow
475 geophysics. Geophys. J. Int. (2016) 204, 1662–1677, doi: 10.1093/gji/ggv558

476 Haimberger, R., Hoppe, A., Schäfer, A. 2005. High-resolution seimic survey on the Rhine
477 River in the northern Upper Rhine Graben. Int. J. Earth Sci. 94, 657–668.

478 Helm J. A. 1995. The Natural Seismic Hazard and Induced Seismicity of the European Hot
479 Dry Rock Geothermal Energy Project at Soultz-sous-Fôrets (Bas-Rhin, France),
480 Unpublished PhD thesis, Ecole et Observatoire de Physique du Globe de Strasbourg,
481 France. 197 pp.

482 Heynekamp, M.R., Goodwin, L.B., Mozley, P.S., Haneberg, W.C. 1999. Controls on fault-
483 zone architecture in poorly lithified sediments, Rio Grande Rift, New Mexico:
484 implications for fault-zone permeability and fluid flow. In: Haneberg, W.C., Mozley, P.S.,
485 Moore, J.C., Goodwin, L.B. (Eds.), Faults and Subsurface Fluid Flow in the Shallow
486 Crust. American Geophysical Union Geophysical Monograph, 113, 27-49.

487 Illies, J. H., and Greiner, G., 1979. Holocene movements and state of stress in the
488 Rhinegraben rift system. Tectonophysics 52, 349-359.

489 Illies J. H. 1981. Mechanism of graben formation. Tectonophysics, 73, 249-266.

490 Kervyn, F., M. Ferry, P. J. Alasset, E. Jacques, and M. Meghraoui. 2002. The potential for
491 large earthquakes in intraplate Europe: the contribution of remote sensing, EGS Meeting
492 With Abstract (Poster), Nice, France.

493 Lemeille F., Cushing M. E., Cotton F., et al. 1999. Evidence for Middle to Late Pleistocene
494 faulting within the northern Upper Rhine Graben (Alsace Plain, France). Earth and
495 Planetary Science, 328, 839-846.

496 Leonard, M. 2010. Earthquake Fault Scaling: Self-Consistent Relating of Rupture Length,
497 Width, Average Displacement, and Moment Release, Bull. Seism. Soc. America 100, No.
498 5A, pp. 1971–1988, doi: 10.1785/0120090189.

499 Leydecker, G. 2009. Earthquake Catalogue for the Federal Republic ofGermany and Adjacent
500 Areas for the Years 800–2002—Datafile, http://www.bgr.de/quakecat — Federal Institute
501 for Geosciences and Natural Resources. Hannover, Germany.

502 Masson, F., Knoepfler, A., Mayer, M., Ulrich, P., Heck, B. 2010, Upper bounds of
503 deformation in the Upper Rhine Graben from GPS data - First results from GURN
504 (GNSS Upper Rhine Graben Network), EGU General Assembly 2010, held 2-7 May,
505 2010 in Vienna, Austria, p.4516.

506 Meghraoui M., Delouis B., Ferry M., et al. 2001. Active normal faulting in the upper Rhine
507 graben and paleoseismic identification of the 1356 Basel earthquake. Science, 293, 2070-
508 2073.

509 Meghraoui M., Camelbeeck T., Vanneste K., et al. 2000. Active faulting and paleoseismology
510 along the Bree fault, lower Rhine graben, Belgium. J. Geophys. Res., 105, 13809-13841.

511 Monninger, R., 1985, Neotektonische bewegungsmechanismen in mittleren Oberrheingraben,
512 PhD Thesis dissertation, Fakultät von Bio- und Geowissenschaften, pp. 219.

513 Nivière et al. 2008. Active tectonics of the southeastern Upper Rhine Graben, Freiburg area
514 (Germany). Quaternary Science Review, 27, 541-555.

515 Okada,Y. 1985. Surface deformation due to shear and tensile faults in a half-space. Bull.
516 Seismol. Soc. Am., 75, 1135–1154.

517 Petrik, A., Beke, B., & Fodor L. 2014. Combined analysis of faults and deformation bands
518 reveals the Cenozoic structural evolution of the southern Bükk foreland (Hungary).
519 Tectonophysics, 633, 43–62.

520 Peters G., Buchmann T.J., Connolly P., van Balen R. T., Wenzel F., Cloetingh S. 2005.
521 Interplay between tectonic, fluvial and erosional processes along the Western Border Fault
522 of the northern Upper Rhine Graben, Germany. Tectonophysics, 406, 39-66.

523 Peters, G., 2007, Active tectonics in the upper Rhine graben, PhD dissertation, Free
524 University of Amsterdam, pp. 270.

525 Plenefisch, T. and K.-P. Bonjer. 1997. The stress field of the Rhine Graben area inferred from
526 earthquake focal mechanisms and estimation of frictional parameters. Tectonophysics,
527 275, 71-97.

528 Rawling, G.C., Goodwin, L.B. 2003. Cataclasis and particulate flow in faulted, poorly
529 lithified sediments. Journal of Structural Geology, 25, 317-331.

530 Rawling, G.C., Goodwin, L.B. 2006. Structural record of the mechanical evolution of mixed
531 poorly lithified sediments, Rio Grande rift, New Mexico. Journal of Structural Geology,
532 28, 1623-1639.

533 Rawling, G.C., Goodwin, L.B., Wilson, J.L., 2001. Internal architecture, permeability
534 structure, and hydrologic significance of contrasting fault-zone types. Geology 29, 43-46.

535 Saillet E. and Wibberley C.A.J. 2010. Evolution of cataclastic faulting in high-porosity
536 sandstone, *Bassin du Sud-Est*, Provence, France. Journal of Structural Geology, 32,
537 1590–1608 doi:10.1016/j.jsg.2010.02.007

538 Schultz, R.A., and Siddharthan, R., 2005, A general framework for the occurrence and
539 faulting of deformation bands in porous granular rocks: Tectonophysics, v. 411, p. 1–18,
540 doi: 10.1016/j.tecto.2005.07.008.

541 Sigda, J.M., Goodwin, L.B., Mozley, P.S., Wilson, J.L. 1999. Permeability alteration in small-
542 displacement faults in poorly lithified sediments: Rio Grande Rift, Central New Mexico.
543 In: Haneberg, W.C., Mozley, P.S., Moore, J.C., Goodwin, L.B. (Eds.), Faults and
544 Subsurface Fluid Flow in the Shallow Crust. American Geophysical Union Geophysical
545 Monograph, 113, 51-68.

546 Sisfrance, Seismicity catalogue of France, http://www.sisfrance.net, last accessed 18 June
547 2015.

548 Stein, S., Liu, M., Camelbeeck, T., Merino, M., Landgraf, A., Hintersberger, E., & Kuebler,
549 S., 2015, Challenges in assessing seismic hazard in intraplate Europe: in Landgraf, A.,
550 Kuebler, S., Hintersberger, E.& Stein, S. (eds), Seismicity, Fault Rupture and Earthquake
551 Hazards in Slowly Deforming Regions. Geological Society, London, Special
552 Publications, 432, doi :org/10.1144/SP432.7

553 Vanneste, K., Verbeeck, K., Camelbeeck, T., Renardy, F., Meghraoui, M., Jongmans, D.,
554 Paulissen, E., and Frechen, M., 2001, Surface rupturing history of the Bree fault
555 escarpment, Roer valley graben: New trench evidence for at least six successive events
556 during the last 150 to 185 kyr: Journal of Seismology, v. 5, p. 329–359, doi:
557 10.1023/A:1011419408419.

558 Weidenfeller, M. and Zöller, L., 1995. Mittelpleistozäne tektonik in einer Lös-Paläoboden-
559 Abfolge am westlichen Rand des Oberrheingraben. Mainzer geowiss.Mitt. 24, 87-102.

560
561
562
563
564

565 **Figure Captions**

566

567 Fig. 1. The Upper Rhine Graben instrumental and historical seismicity: blue circles are
568 seismicity from 1960 to 2012 and yellow boxes are seismicity from AD 800 to 1960
569 (Leydecker, 2009 and SiHex catalogue, Cara et al., 2015). Note the location of the 1952
570 earthquake sequence (light brown; Leydecker, 2009). The box outlines the location of Fig. 2a.
571 The topography is an extract of the SRTM 3-arc-second (~90 m) posting digital elevation
572 model (Farr and Kobrick, 2000). The inset shows the study area in continental Europe.
573
574 Fig. 2. a) Tectonic morphology using SRTM digital topography (see Fig. 1 for location) along
575 the western URG and location of the Riedseltz fault (black arrows). The Reidseltz fault joins
576 the Worms fault scarp (WFS) to the north. This fault zone crosses the Riedseltz quarry (box is
577 for geological map of Fig. 2d) and extends to the north towards Worms and Wacheheim. The
578 red arrows mark the location of a possible parallel fault branch and related scarp. The dashed
579 line is location of seismic profile of figures 2 b and c.
580 b) Seismic profile (commercial) and c) interpreted seismic profile with illustrated fault offsets
581 at depth. Located immediately east of Wissembourg, the profile displays normal faults that
582 seem to reach the surface and affect Oligocene-Miocene units at depth (green and orange
583 layers). Note the slight vertical exaggeration so the fault dips are about 70° to 80°.
584 d) Geological map of the southern extension of Riedseltz fault and quarry area. 1: Sandstone
585 and clay of the Trias Substratum of the Vosges mountains; 2: Clay units of Oligocene, 3:

Pliocene sandy clay and gravel deposits, 4: Late Quaternary alluvial sand, gravel and loess (Riss and Würm), 5: Holocene colluvial and alluvial deposits, 6: Peat of marsh areas with sandy-silt alluvial units, 7: Neogene and Quaternary fault, 8: Late Quaternary and Holocene fault scarp (seismogenic fault zone).

Fig. 3. a) Panorama of the Riedseltz quarry showing nature of quarry host units and position of fault (white arrows). Seated figure to the right of the fault for scale.
b) Interpretive sketch of fault zone next to c) field photograph. The grey lines in b) indicate the geometry of the cataclastic deformation bands. The black crosses are markers at 1 m grid spacing on the outcrop – note that the grid in c) is distorted due to the 3D nature of the outcrop face. Inset stereonet (lower hemisphere) shows the geometry of fault and bedding planes.

Fig. 4. Details of hand specimens. a) Deformation bands are the paler bands about 1mm wide running vertically in this image. They split about half way up this sample with an anastomosing geometry common in deformation bands (Fossen et al 200). They are marginally more consolidated than the sediment around them and stand slightly proud of the surface.
b) View onto a slip surface face showing streaked out oxides along the slip surfaces. The streaks are oriented vertically in this figure.

Fig. 5. Deformation bands with reduced grain size. a) whole thin section showing deformation bands running right to left. Note the mottled colour staining at the bottom of the thin section. Arrow shows location for sampling in b and c. Scale bar = 1cm. b) Plain polarised light (scale bar 1 mm across), and c) backscatter electron SEM image of deformation band from this section, showing intense grain size reduction along the margin.

Fig 6. SEM backscatter images of spalling (sp) at grain margins and transgranular fractures (tg). Note the later coating of clay around the grains, which post-dates the spalling.

Fig. 7. Typical colour variations of the matrix. a) Clay matrix in plain polarised light, and b) Backscatter SEM, note the reduced grain size. c) Boundary between region of Fe-oxide matrix and clay matrix and (d) Fe-oxide matrix with clay filled fracture (arrowed), few fine grains and little/no grain contacts. Photomicroscope images are plain polarised light and the scale bars are 1 mm across.

Fig. 8. XRD data for samples from the footwall (top, black traces), hangingwall (middle, grey traces) and fault zone (bottom, black traces). The fault zone seems enriched in halite and to have reduced kaolinite with respect to the host rocks.

Fig. 9. a) EDX element map of the deformation bands shows iron-rich cement concentrated in fine grained layers (Green = Fe; Red = Ca; Blue = Al). Iron concentration is not always along slip-surfaces. b) Backscatter SEM image of the same area.

Fig. 10. Dislocation model (using Okada, 1985) applied to the 25-km-long fresh scarp of the Riedseltz normal fault segment (strike: 15°N, Dip: 75 east, rake: -90, average slip: 0.6 m; see also Fig. 2b), suggesting an earthquake magnitude Mw 6.64. Black box is Riedseltz quarry location.

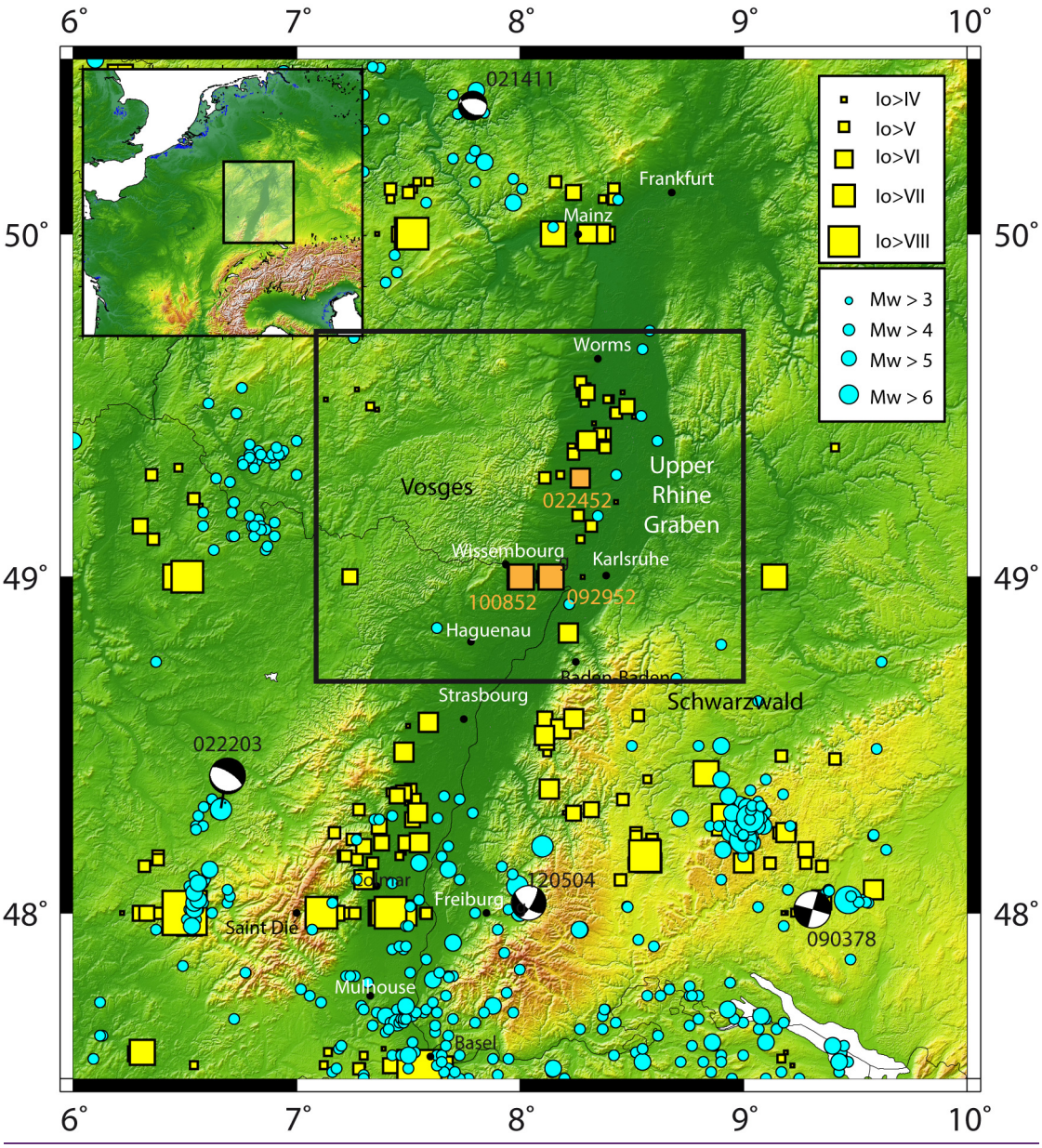
6°
7°
8°
9°
10°
50°
49°
48°
Io>IV
Io>V
Io>VI
Io>VII
Io>VIII
Mw > 3
Mw > 4
Mw > 5
Mw > 6
021411
Frankfurt
Mainz
Worms
Vosges
Upper
Rhine
Graben
022452
Wissembourg
Karlsruhe
100852
092952
Haguenau
Baden-Baden
Strasbourg
Schwarzwald
022203
Colmar
120504
Freiburg
Saint Die
090378
Mulhouse
Basel

635

636

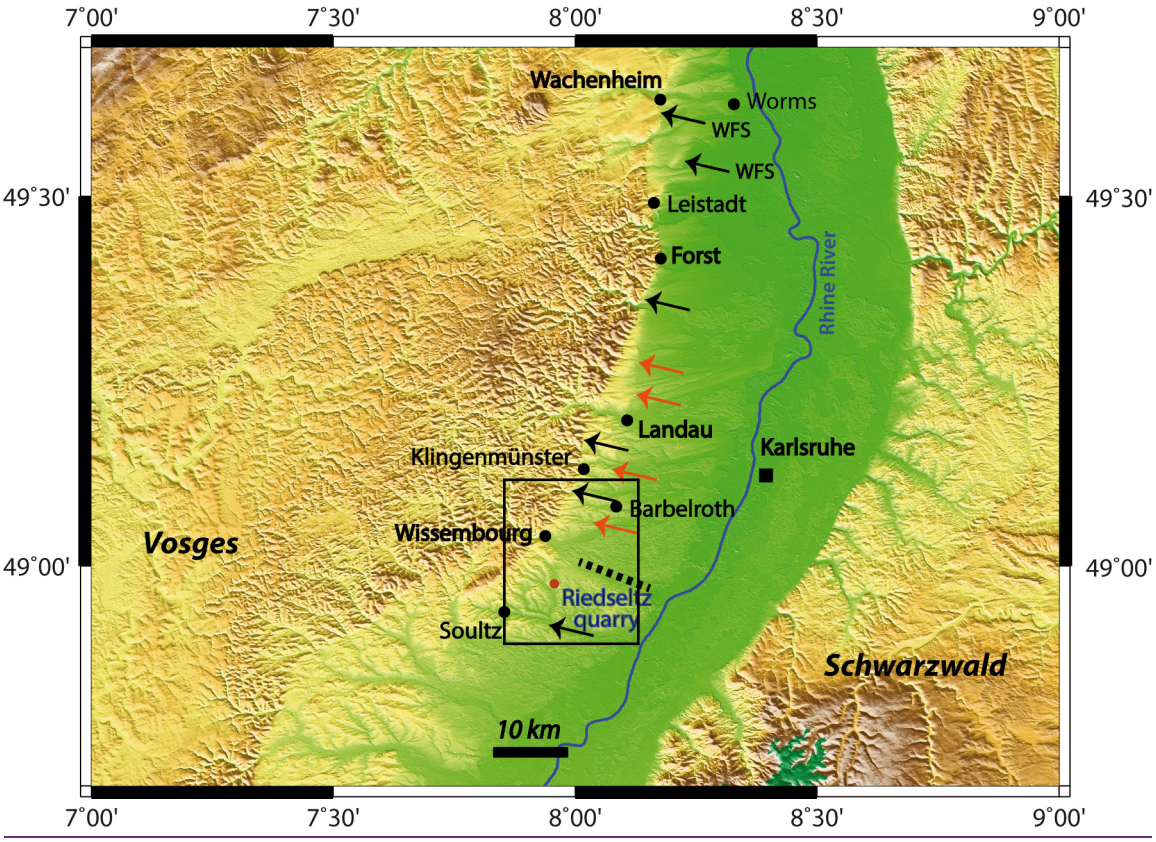
7°00'
7°30'
8°00'
8°30'
9°00'
49°30'
49°00'
Wachenheim
Worms
WFS
WFS
Leistadt
Forst
Rhine River
Landau
Karlsruhe
Klingenmünster
Barbelroth
Wissembourg
Vosges
Riedseltz
quarry
Soultz
Schwarzwald
10 km

637

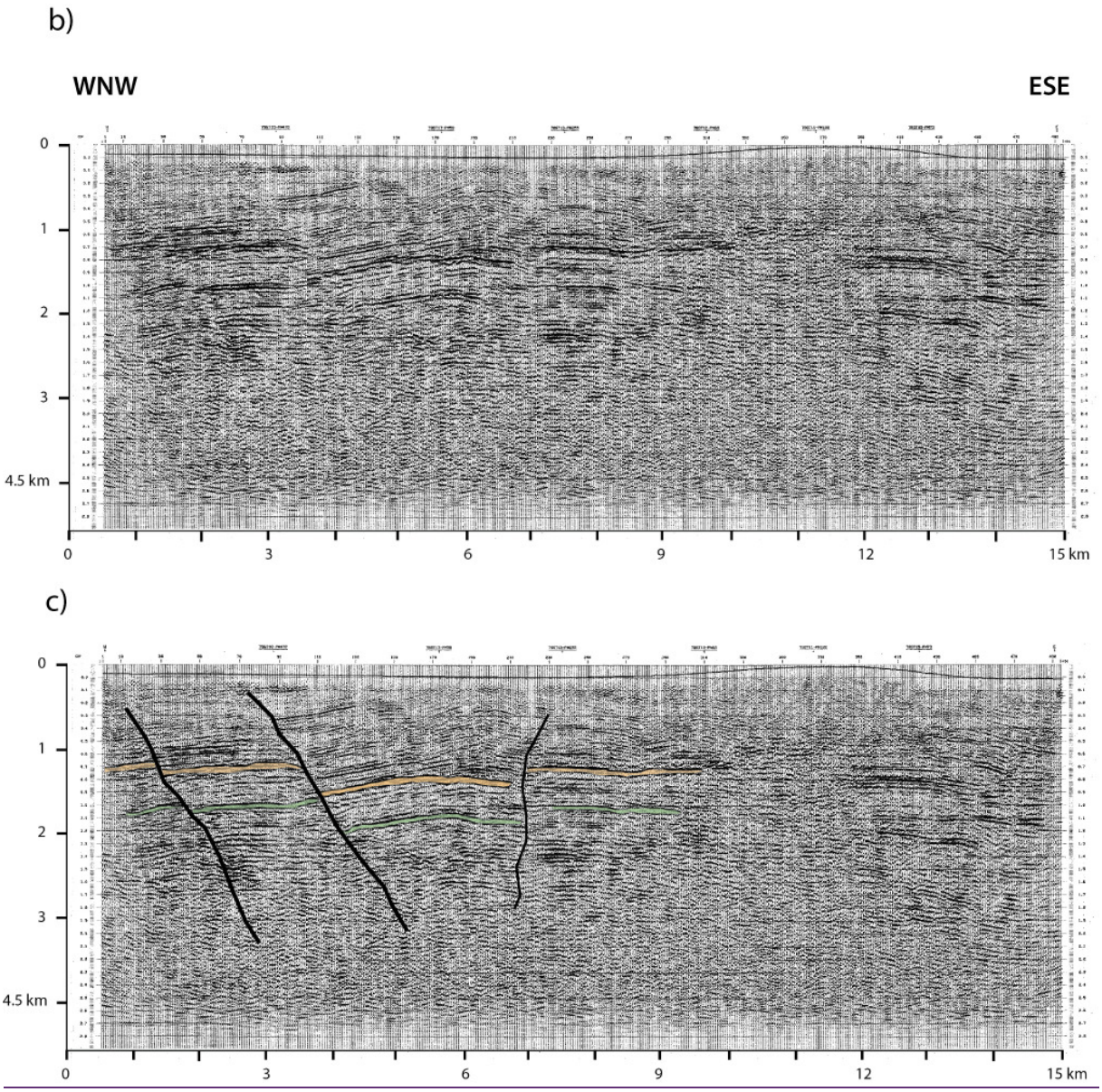

638

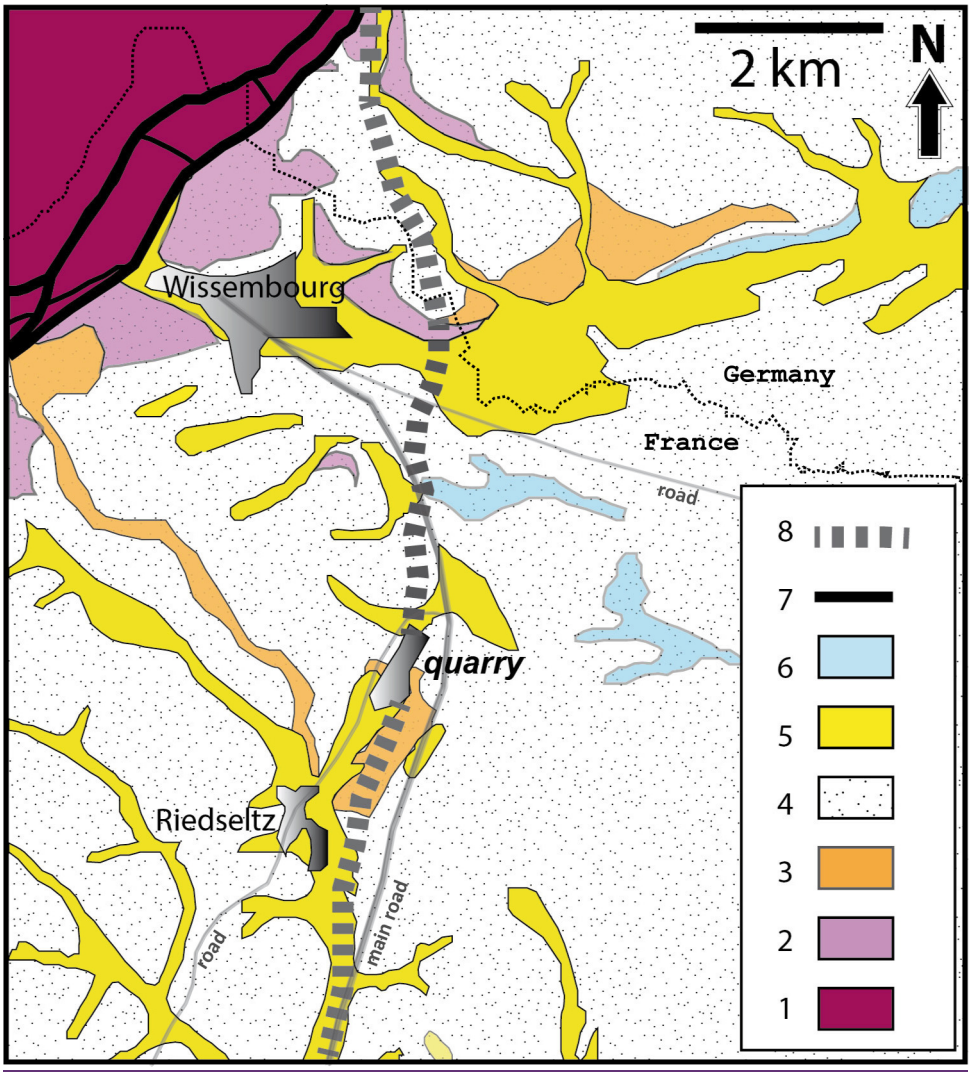
2 km
N
Wissembourg
Germany
France
road
quarry
Riedseltz
road
main road
8
7
6
5
4
3
2
1

639

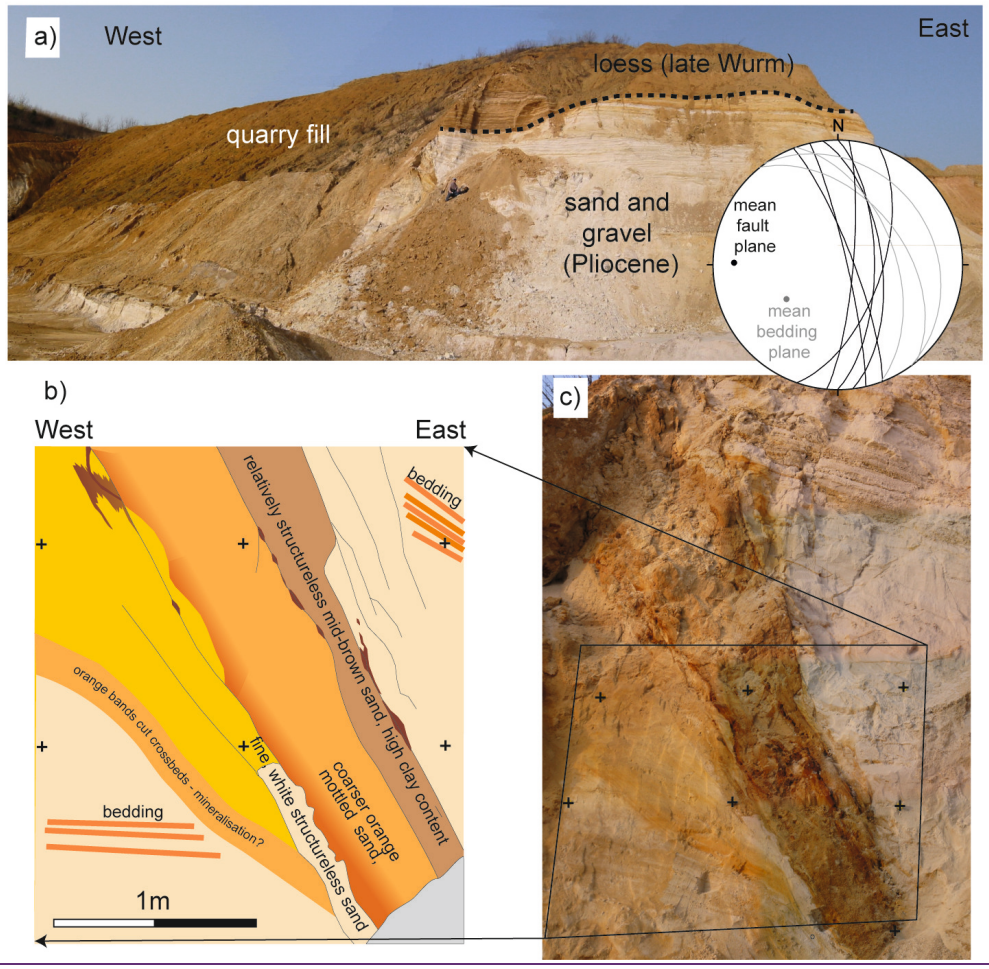
a)
West
East
loess (late Wurm)
quarry fill
sand and
gravel
(Pliocene)
N
mean
fault
plane
mean
bedding
plane
b)
West
East
bedding
relatively structureless mid-brown sand, high clay content
orange bands cut crossbeds - mineralisation?
fine, white structureless sand
coarser orange
mottled sand,
bedding
1m
c)

640

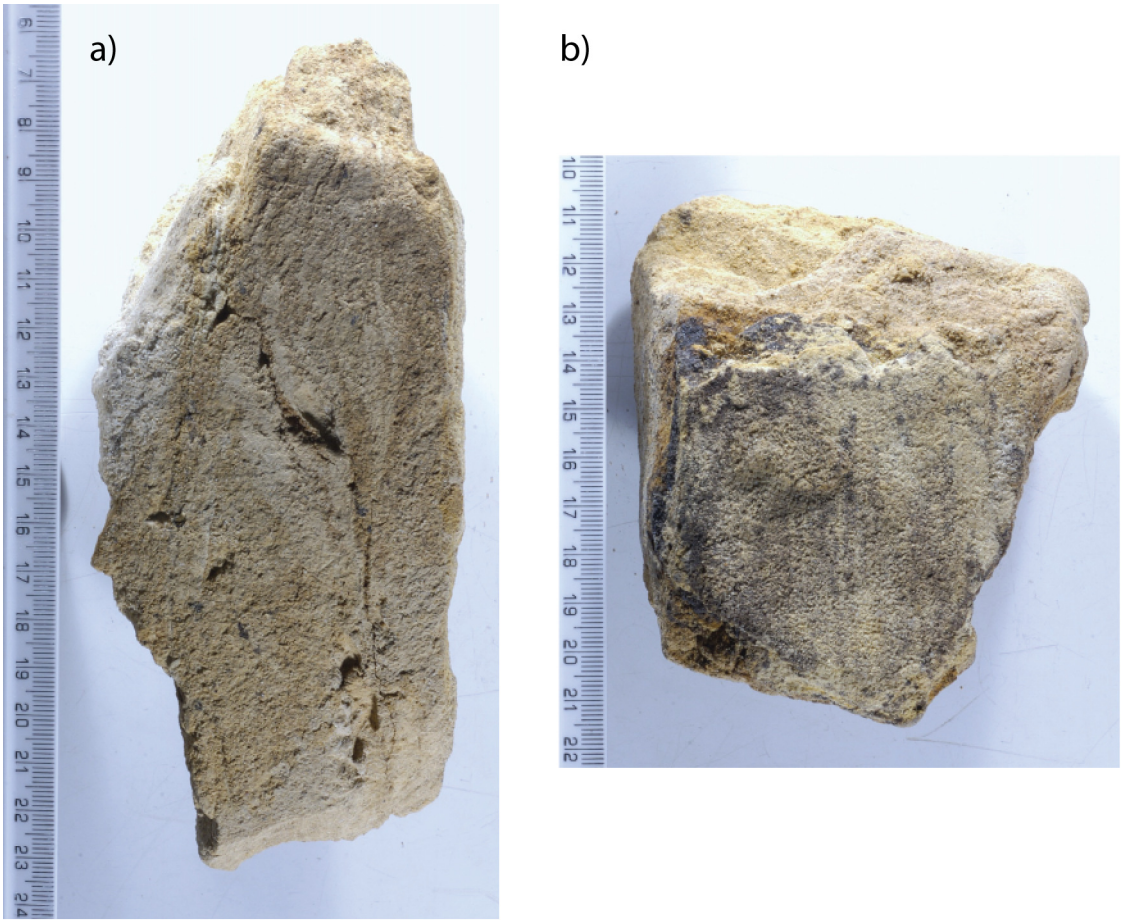

641

642

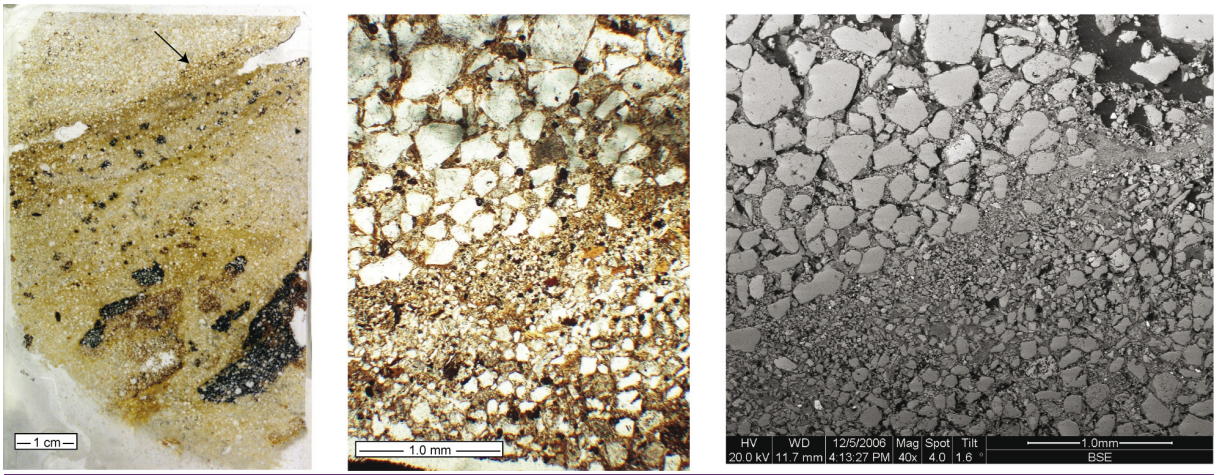
1 cm
1.0 mm
HV 20.0 kV
WD 11.7 mm
12/5/2006 4:13:27 PM
Mag 40x
Spot 4.0
Tilt 1.6 °
1.0mm
BSE

643

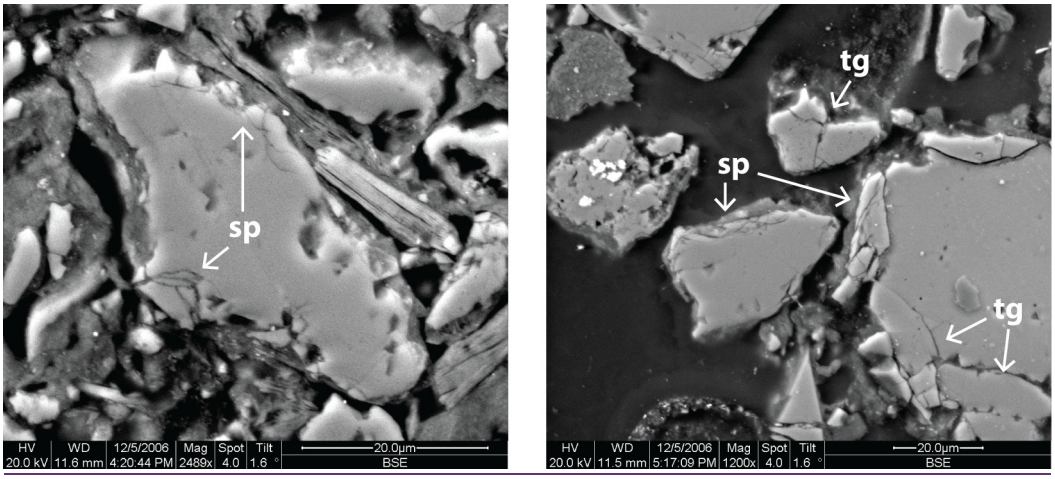
sp
HV WD 12/5/2006 Mag Spot Tilt 20.0µm
20.0 kV 11.6 mm 4:20:44 PM 2489x 4.0 1.6 ° BSE
tg
sp
tg
HV WD 12/5/2006 Mag Spot Tilt 20.0µm
20.0 kV 11.5 mm 5:17:09 PM 1200x 4.0 1.6 ° BSE

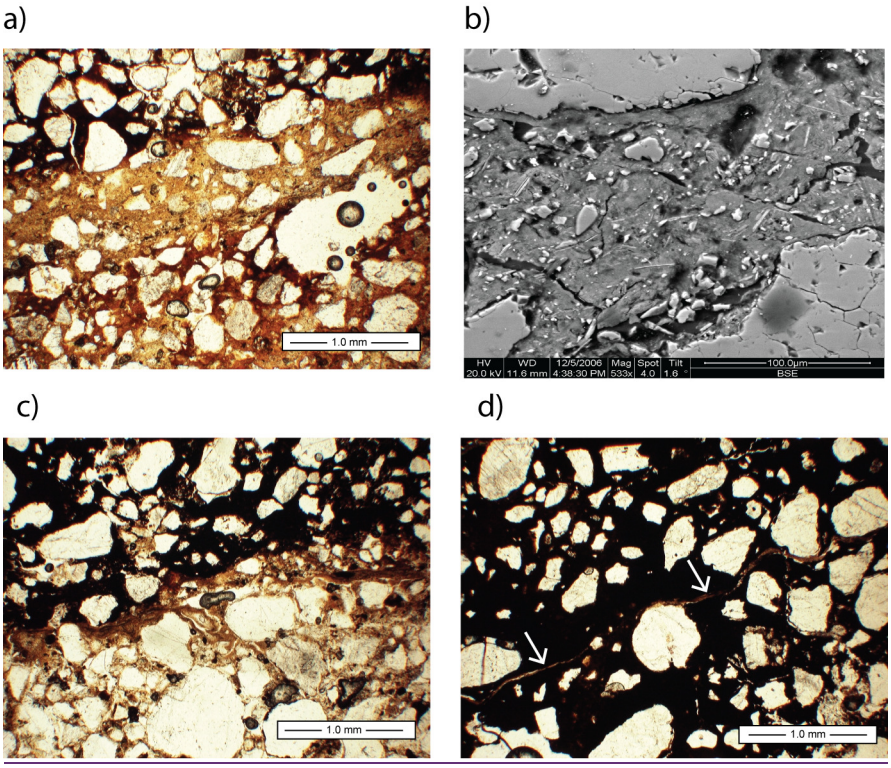
a)
b)
1.0 mm
HV WD 12/5/2006 Mag Spot Tilt
20.0 kV 11.6 mm 4:38:30 PM 533x 4.0 1.8
100.0µm
BSE
c)
d)
1.0 mm
1.0 mm

644

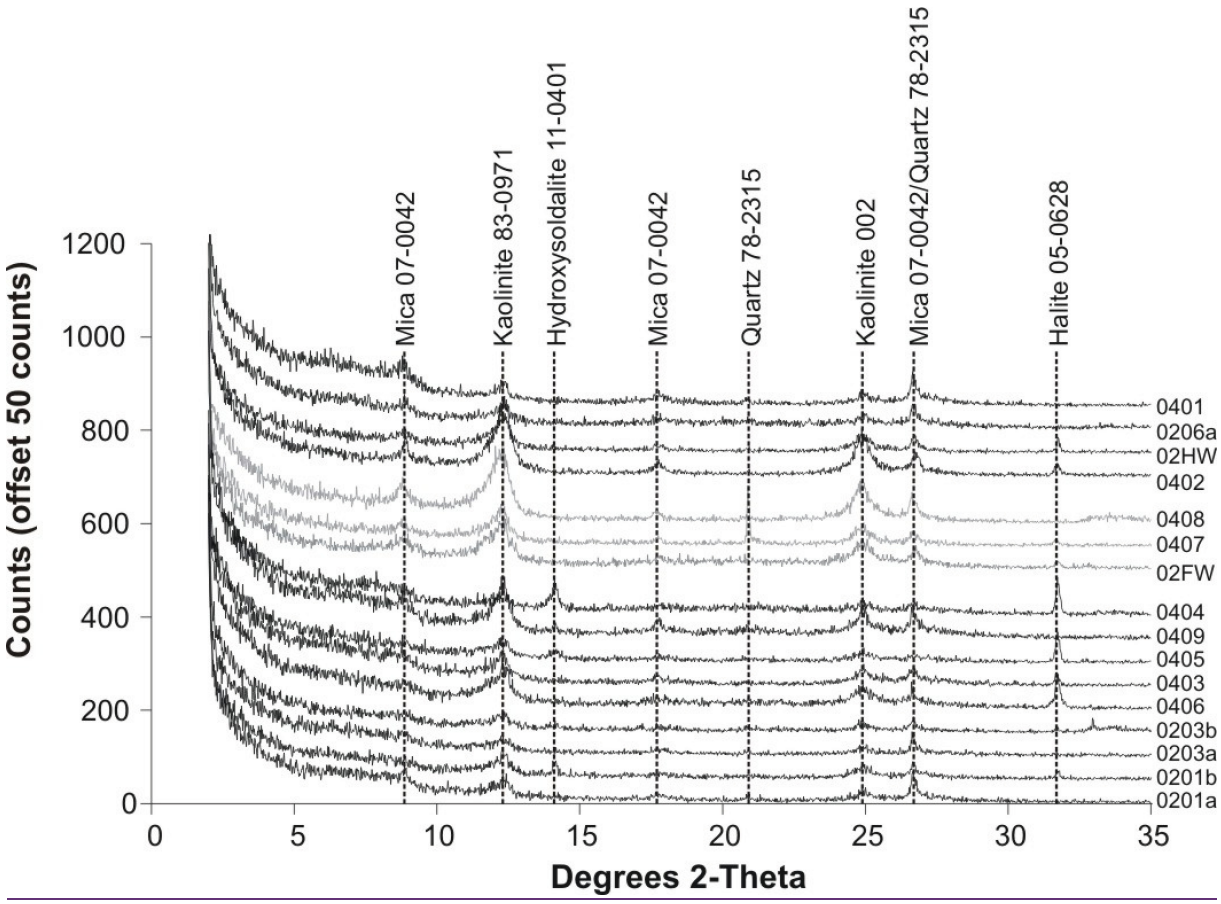
Mica 07-0042
Kaolinite 83-0971
Hydroxysoldalite 11-0401
Mica 07-0042
Quartz 78-2315
Kaolinite 002
Mica 07-0042/Quartz 78-2315
Halite 05-0628
Counts (offset 50 counts)
Degrees 2-Theta
0401
0206a
02HW
0402
0408
0407
02FW
0404
0409
0405
0403
0406
0203b
0203a
0201b
0201a

645

a)

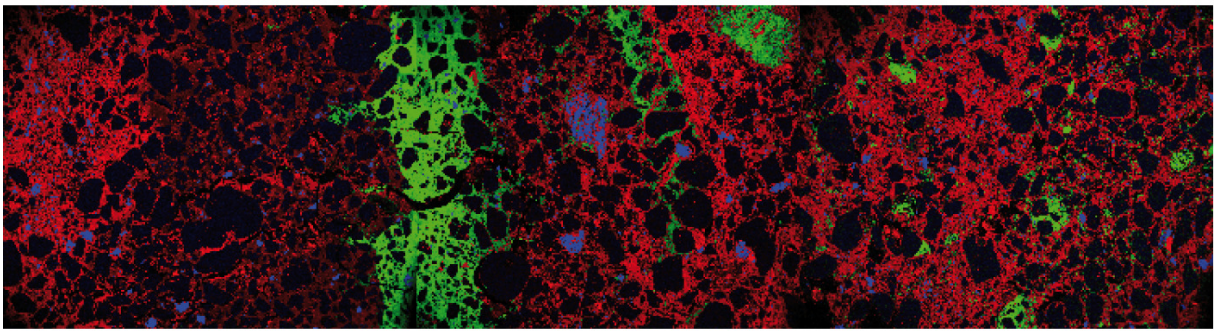

b)

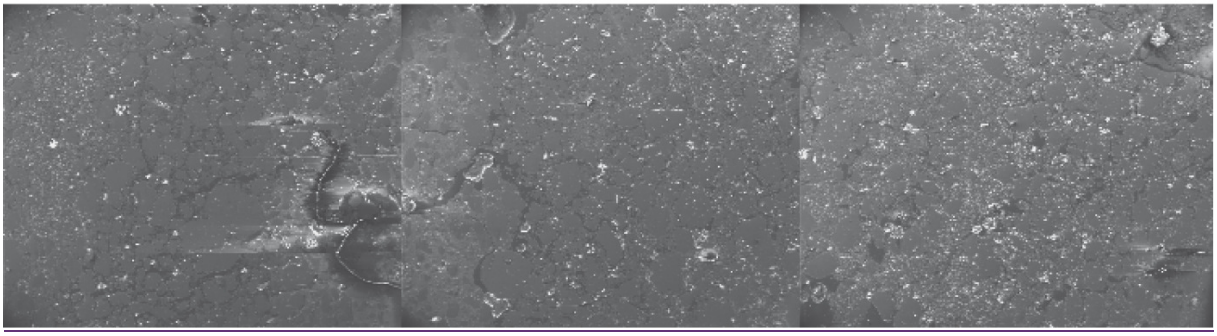

646

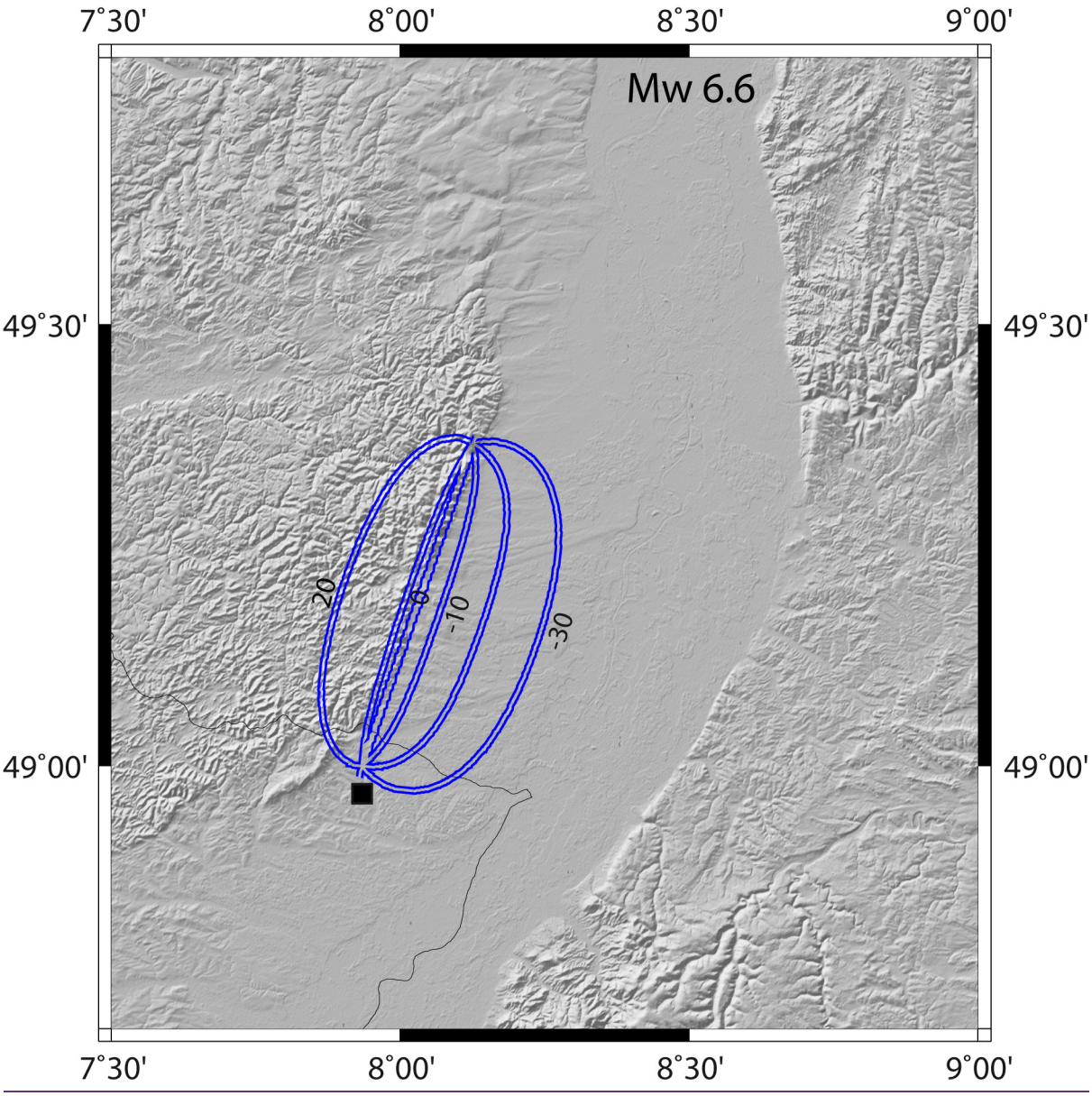

647